© 2022. Published by The Company of Biologists Ltd | Development (2022) 149, dev200750. doi:10.1242/dev.200750

RESEARCH ARTICLE

Dbx1 controls the development of astrocytes of the intermediate spinal cord by modulating Notch signaling

Maria Micaela Sartoretti, Carla A. Campetella and Guillermo M. Lanuza*

ABSTRACT

Significant progress has been made in elucidating the basic principles that govern neuronal specification in the developing central nervous system. In contrast, much less is known about the origin of astrocytic diversity. Here, we demonstrate that a restricted pool of progenitors in the mouse spinal cord, expressing the transcription factor Dbx1, produces a subset of astrocytes, in addition to interneurons. Ventral p0-derived astrocytes (vA0 cells) exclusively populate intermediate regions of spinal cord with extraordinary precision. The postnatal vA0 population comprises gray matter protoplasmic and white matter fibrous astrocytes and a group of cells with strict radial morphology contacting the pia. We identified that vA0 cells in the lateral funiculus are distinguished by the expression of reelin and Kcnmb4. We show that Dbx1 mutants have an increased number of vA0 cells at the expense of p0-derived interneurons. Manipulation of the Notch pathway, together with the alteration in their ligands seen in Dbx1 knockouts, suggest that Dbx1 controls neuron-glial balance by modulating Notch-dependent cell interactions. In summary, this study highlights that restricted progenitors in the dorsal-ventral neural tube produce region-specific astrocytic subgroups and that progenitor transcriptional programs highly influence glial fate and are instrumental in creating astrocyte diversity.

KEY WORDS: Astrocytes, Spinal cord, Glia, Transcription factor, Progenitor, Specification

INTRODUCTION

Astrocytes, oligodendrocytes and ependymocytes represent about 60% and 75% of spinal cord cells in rodents and humans, respectively (Bjugn and Gundersen, 1993; Fu et al., 2013; Bahney and von Bartheld, 2018). Astrocytes play crucial supportive and active roles in the organization and functioning of the nervous system. They maintain the blood–brain barrier, adjust the distribution of ions and protons, and regulate the water balance. They are also key in the formation, function and plasticity of neural networks by adjusting calcium fluxes, providing neurotransmitter precursors, producing neuropeptides and trophic support factors, and modulating synaptic assembly and transmission (Allen and Eroglu, 2017; Barres, 2008; Verkhratsky and Nedergaard, 2018).

During neural tube development, glial cells are produced from ventricular zone (vz) progenitors that previously generated neurons (Rowitch and Kriegstein, 2010). Substantial advances have been reached in understanding the gene-regulatory programs that control neurogenesis and neuronal diversity in the embryonic spinal cord. It is well established that morphogens pattern the dorsal-ventral (DV) axis of the neural tube, and induce the expression of a combination of transcription factors in spatially limited territories subdividing the neuroepithelium into 11 progenitor domains (Briscoe et al., 2000; Jessell, 2000; Balaskas et al., 2012; Lek et al., 2010; Sagner and Briscoe, 2019). These DV-restricted progenitors (p0-p3, pMN and dp1-6), produce distinct cardinal classes of spinal neurons, ventral V0-V3, motoneurons, and dorsal dI1-dI6 and dILA/B (Lai et al., 2016; Lu et al., 2015; Sagner and Briscoe, 2019).

After neurogenesis, the remaining progenitor cells in the vz start to generate astrocyte and oligodendrocyte precursors (Rowitch and Kriegstein, 2010). Together with this switch in competence, the neuroepithelium undergoes changes in gene expression and a phenotypical transformation into radial glia (Barry and McDermott, 2005; Deneen et al., 2006; Stolt et al., 2003; Kang et al., 2012; Freeman, 2010). Glial cell production also follows DV regional organization. Oligodendrocytes, which populate the entire spinal cord, derive from the ventral pMN/pOL and dorsal domains (Zhou et al., 2000; Lu et al., 2000; Cai et al., 2005; Vallstedt et al., 2005; Fogarty et al., 2005). Astrocytes, however, are produced from vz territories spanning the whole DV axis (Rowitch and Kriegstein, 2010; Pringle et al., 2003).

In contrast with the deep knowledge attained on neuronal cell-type specification, the comprehension of the developmental principles behind astrocyte specification and diversity is more limited. Recent studies in the embryonic spinal cord and brain indicate that astrocyte development follows a segmental template similar to that involved in early neuron production (Tsai et al., 2012; Vue et al., 2014; Molofsky et al., 2014; Herrero-Navarro et al., 2021).

In the ventral and dorsal spinal cord, different progenitor domains contribute to astrocyte subtypes, which are allocated to spatial regions in accordance with their embryonic origin (Tsai et al., 2012; Hochstim et al., 2008; Vue et al., 2014). At least three molecularly distinct subtypes of ventral astrocytes (vA1, vA2 and vA3) were identified based on the combinatorial expression of the axon guidance and migration proteins Slit1 and reelin (Hochstim et al., 2008). The spatial arrangement of these populations within the spinal cord gray (GM) and white (WM) matter correlates with their ventricular source (p1, p2 and p3, respectively) (Hochstim et al., 2008; Tsai et al., 2012). In addition, key transcription factors of the gene regulatory networks that control neuron diversification also contribute to astrocyte specification and heterogeneity in the spinal cord. For instance, the basic helix-loop-helix protein Tal1 is necessary and sufficient for the development of astrocytes and the suppression of oligodendrocyte fate in p2 progenitors (Muroyama et al., 2005). Similarly, deletion and forced expression of Pax6 and

Developmental Neurobiology Lab, Fundación Instituto Leloir and Consejo Nacional de Investigaciones Científicas y Técnicas (IIBBA-CONICET), Avenida Patricias Argentinas 435, Buenos Aires 1405, Argentina.

*Author for correspondence (GLanuza@Leloir.org.ar)

M.M.S., 0000-0003-1465-6337; C.A.C., 0000-0003-2061-5128; G.M.L., 0000-0003-3311-2263

Handling Editor: François Guillemot
Received 13 March 2022; Accepted 27 June 2022

Development (2022) 149, dev200750. doi:10.1242/dev.200750

Nkx6-1 disrupt the molecular identity of astrocyte subsets in the ventral and ventro-lateral WM (Hochstim et al., 2008; Zhao et al., 2014). Despite this progress, our understanding of the molecular and functional astrocytic heterogeneity across central nervous system regions is far from complete.

Here, we describe the specification, migration and maturation of a spinal cord astrocyte population originating from Dbx1-expressing vz progenitors of the p0 domain. Through cell-fate tracings, we show that ventral p0-derived astrocytes (vA0 cells) are settled in remarkably precise and reproducible positions to cover the intermediate portion of the mouse spinal cord. This cell group is morphologically heterogeneous and comprises protoplasmic-like astrocytes in the GM, fibrous WM astrocytes and radial astrocytes at the subpial surface.

We further show that in the absence of Dbx1, p0 cells give rise to a significantly increased number of astrocytes, which are produced at the expense of V0 interneurons. We provide evidence that Dbx1 controls the appropriate size of the p0-derived populations by modulating Notch signaling efficacy within the p0 domain and thus coordinating region-specific cell-fate developmental features.

RESULTS

Dbx1$^+$ progenitors produce glial cells that populate the medial-lateral spinal cord

The transcription factor Dbx1 is expressed in a discrete domain of the neural tube (Fig. 1A). To determine the complete contribution of Dbx1-expressing progenitors to spinal cord cell types, we used *Dbx1^{lacZ}* mice, in which nuclear β-galactosidase (β-gal) recapitulates Dbx1 expression and its stability allows for accurate fate mapping (Fig. 1A,B, Fig. S1A-C; Pierani et al., 2001; Lanuza et al., 2004; Bouvier et al., 2010). At embryonic day (E) 13.5, the end of the neurogenic period, V0 interneurons were established in the ventromedial spinal cord (Fig. 1C). Remarkably, at E18.5 a different cohort of β-gal$^+$ cells was seen in the intermediate region of the spinal cord (Fig. 1D, arrow). This group of cells had a thinner nuclear shape (Fig. 1E,F, Fig. S1D-F) and a specific expression profile. They were negative for neuronal NeuN (Rbfox3) and expressed Sox2 (Fig. 1G-J), a transcription factor that is active in progenitors and glial cells (Hoffmann et al., 2014).

Quantitative distribution analyses of β-gal$^+$,Sox2$^+$ cells revealed that p0-derived glia colonize a precise region of the spinal cord. β-gal$^+$,Sox2$^+$ nuclei were observed between the midline and the pial surface, spanning the GM and WM (Fig. 1K, Fig. S1G-L). This territory is different from the V0 location (Fig. 1L, Fig. S1H), indicating that neurons and glia produced by the same vz domain follow dissimilar migration routes. In the hindbrain, p0 cells also generated both neurons and glia, although these were intermingled in the ventrolateral medulla (Fig. S1M-P). To determine whether the precise positioning of Dbx1-derived glia is a transient state followed by later dispersal in the spinal tissue, we analyzed their postnatal location. However, β-gal$^+$ cells at postnatal day (P) 6 and P15 were still restricted to the intermediate region without DV displacement (Fig. 1M, Fig. S1Q).

Lateral β-gal$^+$ cells were only seen at advanced embryonic stages, suggesting they are produced after E13, once neurogenesis has ended. At E13.5, vz Dbx1 spatial expression (Fig. 1N,O, Fig. S1B, R) remained similar to its earlier pattern (Briscoe et al., 2000; Pierani et al., 2001). Staining for transcription factors with DV restriction showed vz β-gal$^+$ cells within Pax6$^+$ territories, dorsal to the Nkx6-1$^+$ domains (Fig. 1N, Fig. S1R). The dorsal patterning gene Pax3 partially overlapped with Dbx1, establishing ventral and

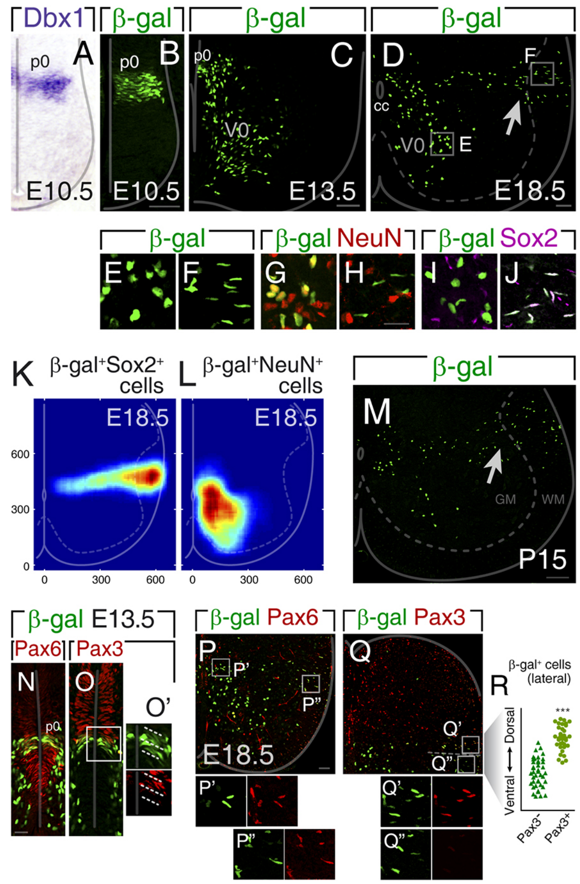

Fig. 1. Dbx1$^+$ p0 progenitors produce glial cells that populate a defined region of the intermediate-lateral spinal cord. (A-J) Dbx1-derived cells in *Dbx1^{lacZ}* mice. (A,B) Transverse E10.5 neural tube sections hybridized with *Dbx1* probe (A) and immunostained against β-gal (B). (C) At E13.5, the β-gal$^+$ population includes V0 interneurons and late progenitors in the p0 domain. (D-J) E18.5 cross-sections showing V0 neurons and a group of β-gal$^+$ cells between the midline and the lateral funiculus (arrow). cc, central canal. (E-J) Dbx1-derived neurons (E,G,I) and β-gal$^+$ lateral cells (F,H,J) have distinctive nuclei morphology, NeuN and Sox2 expression. (K,L) Density maps of β-gal$^+$ cells in E18.5 spinal cord based on the location of 775 Sox2$^+$ and 890 NeuN$^+$ cells. (M) The regional allocation of β-gal$^+$ astroglial cells is maintained postnatally, as seen in P15 spinal cord. (N-O′) E13.5 p0 vz progenitors are Pax6$^+$ and are subdivided into dorsal and ventral pools based on Pax3 expression. White dashed lines in O′ indicate β-gal and Pax3 boundaries. (P-R) DV organization of glial populations at E18.5. β-gal$^+$ cells are Pax6$^+$. β-gal$^+$ cells positioned more dorsally express Pax3 (Q′,R) whereas cells settled ventrally are negative (Q″,R) (***P<0.001, Mann–Whitney test). Vertical gray lines indicate the midline, solid outlines the outer boundary of the spinal cord, and dashed lines the boundary between GM and WM. Scale bars: 50 µm (A-D, P,Q); 20 µm (E-J,N,O); 100 µm (M). See also Fig. S1.

dorsal p0 subdomains (Fig. 1O,O′). At E18.5, β-gal$^+$ glial cells in the GM and WM were Pax6$^+$ (Fig. 1P-P″; ∼96%) and did not express Nkx6-1, which marks more ventral WM cells (Fig. S1S-S″; Hochstim et al., 2008). We also found that 43±4% (mean±s.d.) of Dbx1 progeny is Pax3$^+$ (Fig. 1Q-Q″), with Pax3 limited to more dorsal β-gal$^+$ cells (Fig. 1Q-R). The uneven Pax3 expression strictly correlates with the polarized early Pax3 patterning and indicates that the arrangement of β-gal$^+$ glia closely mirrors their DV vz origins.

In summary, fate mappings indicate that Dbx1$^+$ progenitors produce, in addition to V0 neurons, a population of glial cells that migrate laterally and settle in a specific region of the postnatal spinal cord.

Development (2022) 149, dev200750. doi:10.1242/dev.200750

Dbx1-derived population comprises protoplasmic, fibrous and radial astrocytes

To explore the identity of p0-derived cells, we studied the expression of several molecular markers. In newborn pups, all β-gal$^+$,Sox2$^+$ cells were robustly co-labeled with the astroglial transcription factors Sox9 and Nfia (Deneen et al., 2006; Kang et al., 2012) (Figs 1J and 2A-C,H). The glutamate transporter Glast (Slc1a3), which is restricted to the vz and the astrocytic lineage (Shibata et al., 1997), was expressed in most β-gal$^+$ cells at P0, in line with their astroglial identity (Fig. 2D,H). As shown above, NeuN was not detected in β-gal$^+$ cells in the intermediate-lateral cord (Figs 1H and 2E,H). Given that previous studies have established oligodendrocyte production from dorsal domains (Cai et al., 2005; Fogarty et al., 2005; Vallstedt et al., 2005), we examined whether some β-gal$^+$ cells were oligodendrocyte precursor cells. However, we found they were Olig2 negative (Fig. 2F,H). To confirm the identity of p0-derived cells, we assessed the glial fibrillary acidic protein Gfap, and found that β-gal$^+$ cells within or close to the WM displayed Gfap^{High} processes, whereas those in the GM had very low signal (Fig. 2G,H). The expression of these proteins was also analyzed at P6 and P15, confirming their astrocytic nature. Similar to P0, at P6 and P15, β-gal co-labeled with Sox9, Sox2 and Nfia (Fig. S2A-C, E), but remained NeuN and Olig2 negative (Fig. S2D,G,H). At P15, β-gal$^+$ cells were Gfap positive, with high expression in WM cells (Fig. S2F). Thus, marker analysis indicates that p0 progenitors produce cells that differentiate into astrocytes (vA0).

The glycoprotein reelin is co-expressed with Pax6 in vA1 and vA2 WM astrocytes (Hochstim et al., 2008). As vA0 cells are also Pax6$^+$ (Fig. 1P), we analyzed its presence in the vA0 population, and found that reelin labels WM Dbx1-derived cells (Fig. 2I-J′, Fig. S2I-L). In search of novel vA0 markers, a survey of the Allen Spinal Cord Atlas (http://mousespinal.brain-map.org/) pointed at Kcnmb4, the auxiliary β4-subunit of large conductance Ca^{2+}- and voltage-activated K^+ (BK) channels (Contet et al., 2016), expressed in the lateral funiculus. *In situ* hybridization showed *Kcnmb4* expression in the WM occupied by vA0 cells (Fig. 2K,K′, Fig. S2M). Similar to reelin, *Kcnmb4* expression was limited to WM marginal cells (Fig. 2K,K′). At E13.5, reelin was absent in vz Dbx1$^+$ cells (Fig. S2N), whereas Kcnmb4 was already expressed in the p0 domain (Fig. S2O,P). Hence, reelin and Kcnmb4 are distinctive molecular markers of the vA0 population.

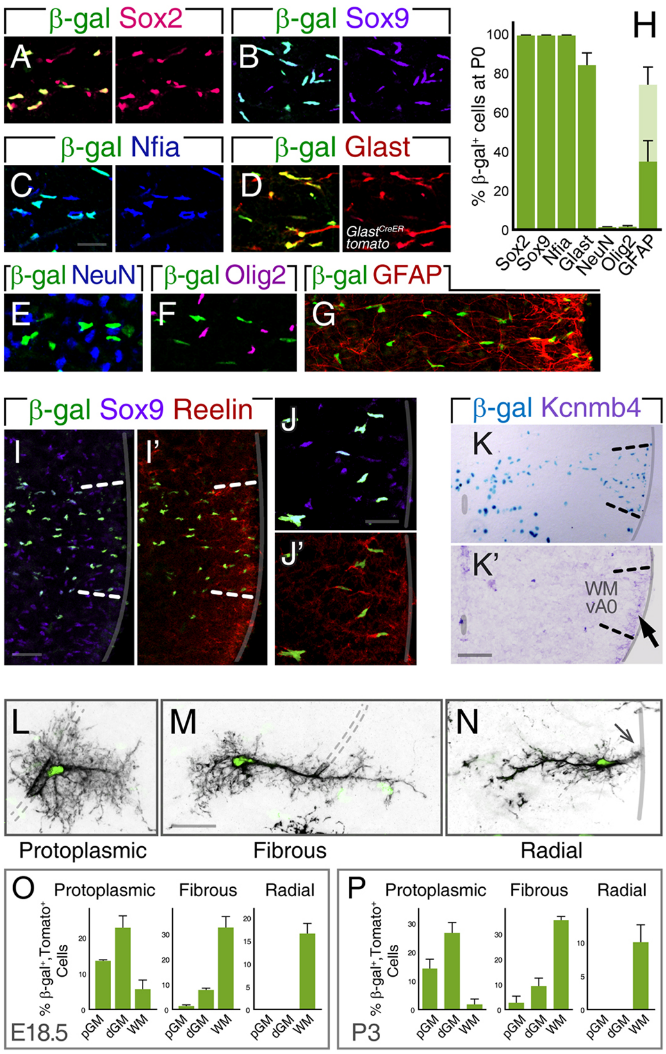

Fig. 2. p0-derived vA0 population is composed of protoplasmic, fibrous and radial astrocytes. (A-H) β-Gal cells in the intermediate spinal cord express astrocytic markers. (A-G) P0 spinal cord stained against β-gal, Sox2, Sox9, Nfia, Glast (*Glast^{CreER};CAG:LSL-tdTomato*, Tam administered at E18.5), NeuN, Olig2 or Gfap. (H) Percentage of β-gal$^+$ cells expressing each protein (12 sections, three cords). Dark and light green bars indicate high and low Gfap levels, respectively. (I-K′) vA0 cells in the WM express reelin and Kcnmb4. (I-J′) P0 cross-sections stained for β-gal, reelin and Sox9. (K) *In situ* hybridization for *Kcnmb4* showing expression in vA0 area close to the pia (arrow). Dashed lines in I,I′,K,K′ indicate vA0 WM territory. (L-P) The vA0 population comprises protoplasmic, fibrous and radial astrocytes. (L-N) Representative examples of Dbx1-derived astroglia at P3. Cells were identified by nuclear β-gal and tomato labeling using *Nestin:CreER;CAG:LSL-tdTomato* mice induced with low dose of Tam at E11.75. Dashed lines demarcate blood vessels, solid gray line delimits the spinal cord and arrow indicates contact with the pia. (O,P) Percentages of β-gal$^+$ cells along the medial-lateral axis (pGM, dGM, WM) at E18.5 and P3 (296 cells from 11 E18.5 embryos and 92 cells from three P3 pups). Scale bars: 20 µm (A-G,I-J′,L-N); 100 µm (K,K′). Values are mean+s.d. See also Fig. S2.

Because vA0 cells are distributed throughout the GM and WM, we evaluated their morphology to determine whether the Dbx1-derived population includes the major classes of astrocytes: protoplasmic and fibrous (Oberheim et al., 2012; Peters et al., 1991). For this purpose, we generated mice carrying the transgene *Nestin:CreER* and the conditional tdTomato reporter and induced scattered recombination in the vz to identify later isolated cells in the parenchyma (Fig. S2Q-R″). There were three major vA0 morphologies at E18.5 and P3. First, 42-43% of β-gal$^+$ cells were protoplasmic-like astrocytes with highly branched bushy processes emanating from their soma (Fig. 2L). Second, 42-47% of vA0 cells were fibrous-like astrocytes with a main straight, long radial process and shorter lateral ramifications (Fig. 2M). We found that both classes have cellular extensions surrounding blood vessels (Fig. 2L,M dashed lines; Tabata, 2015). Finally, 10-16% of β-gal$^+$ cells, the nuclei of which were localized at the subpial surface, displayed a pronounced radial morphology with short transverse processes that contacted the pia (Fig. 2N, arrow) (Liuzzi and Miller, 1987; Petit et al., 2011; Barry and McDermott, 2005).

To define the regions occupied by different vA0 subtypes, the cells were classified according to their medial-lateral location into proximal or distal GM (pGM, dGM) and WM. Consistently, the majority of protoplasmic-like vA0s were in the pGM and dGM (Fig. 2O,P; ∼90%), whereas fibrous-like were mainly in the WM (Fig. 2O,P; ∼80%). Finally, β-gal$^+$ astrocytes with strict radial shape were only settled in the WM close to the pia (Fig. 2O,P). These results demonstrate that Dbx1 progenitors produce a heterogeneous

Development (2022) 149, dev200750. doi:10.1242/dev.200750

population of astrocytes that occupy defined regions of the spinal cord GM and WM.

vA0 precursors derive from radial glia and progressively occupy lateral spinal regions

The experiments described above suggest that astroglia arise from Dbx1$^+$ vz cells after E13.5. Spinal cord neuroepithelial progenitors acquire the radial glia phenotype before becoming the source of glial lineages (Barry and McDermott, 2005). Immunostaining against the radial glia marker nestin revealed that E13.5 β-gal$^+$ ventricular cells radiate long basal processes reaching the basal lamina (Fig. 3A). Additionally, β-gal$^+$ vz cells co-expressed Sox2, Sox9 and Blbp (Fabp7), another radial glia marker (Barry and McDermott, 2005) (Fig. 3B-D). To confirm that the vA0 population derives from radial glia, we analyzed the fate of Dbx1$^+$,Glast$^+$ cells using *Glast^{CreER};tdTomato* conditional reporter mice. Glast appears in spinal cord radial glia slightly preceding the gliogenic period (Shibata et al., 1997). Indelible marking, induced at E13.5, activated recombination in ~90% of germinal zone cells but not in the mantle (Fig. S3A-C). As predicted, at E18.5 we found that β-gal$^+$ cells that migrated laterally, but not V0 neurons, were Tomato$^+$ (~90%; Fig. 3E-E″), demonstrating that Glast$^+$ radial glial cells in the E13.5 p0 domain are the source of vA0 astrocytes.

We next characterized vA0 development in more detail. At E13.5, only a few β-gal$^+$,Sox2$^+$ cells were spotted just outside the vz (Fig. 3F). Later, they gradually occupied more distal positions, reaching the pial surface by E16.5 (Fig. 3F-J). Remarkably, β-gal$^+$, Sox2$^+$ nuclei were restricted to DV intermediate coordinates during development, suggesting exclusive radial migration. At E14.5 and E16.5, β-gal$^+$,Sox2$^+$ cells moving laterally also expressed Sox9 and Nfia (Fig. S3D-H).

To evaluate how Dbx1-derived cells migrate, we studied their shape by mosaic labeling. At E15.5, some β-gal$^+$ cells with thin radial process were still present in the vz (Fig. 3K-L′). In the mantle zone, two contrasting morphologies were seen: some cells with short processes and others with prolonged extensions toward the pia (Fig. 3M,M′, arrowheads). Further analysis at E16.5, when p0 progeny already spans the whole medial-lateral axis, reinforced the presence of two main shapes. First, multipolar cells displaying short ramifications (Fig. 3N) accounted for ~25% and were mainly in the pGM (Fig. 3P). Second, uni/bipolar cells with one extension towards the pia with or without an apically directed process (Fig. 3O) represented ~75% and were predominantly in the dGM and WM (Fig. 3P). The morphology of uni/bipolar cells contacting the pia, together with their soma displacement, are reminiscent of radial migration processes previously described (Nadarajah et al., 2001; Pakan and McDermott, 2014).

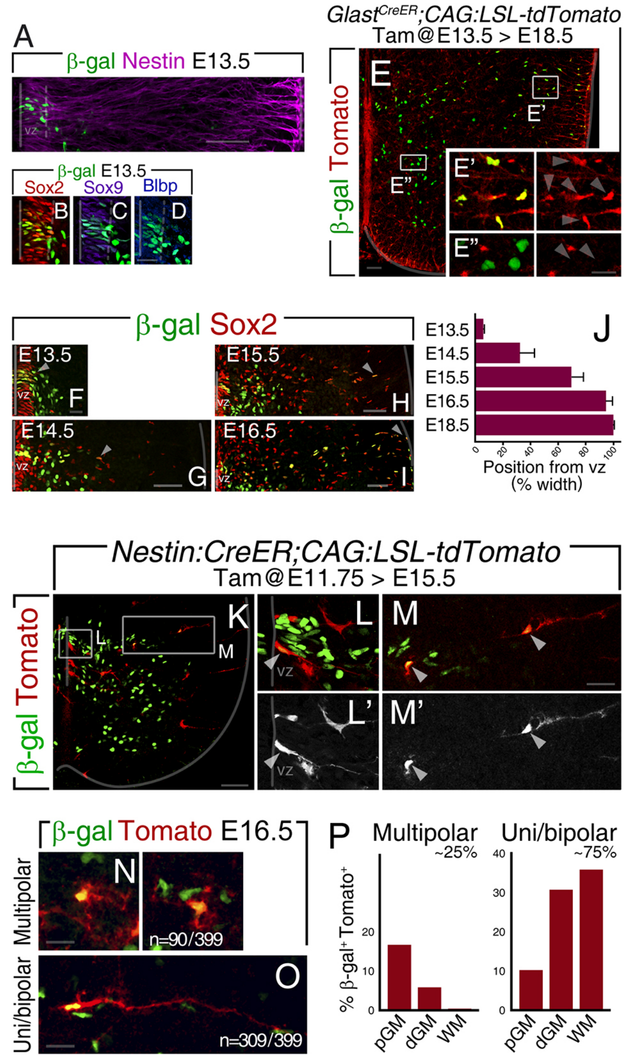

Fig. 3. Dbx1 radial glia give rise to astrocyte precursors that progressively occupy lateral spinal regions. (A-E″) The delayed p0 lineage derives from spinal cord radial glia. (A-D) β-gal, nestin, Sox2, Sox9 and Blbp staining at E13.5. (E-E″) Late-born β-gal$^+$ cells are produced from E13.5 Glast$^+$ progenitors. Tomato labeling in *Glast^{CreER};CAG:LSL-tdTomato* embryos was induced with Tam at E13.5 and analyzed at E18.5. β-gal$^+$ cells in E18.5 lateral spinal cord are tomato$^+$ (89±6%; E′ arrowheads) (653 cells, nine sections, three embryos), whereas V0 neurons are negative (E″, arrowheads). (F-J) Dbx1-derived astroglia progressively occupy distal spinal cord regions. (F-I) Staining of E13.5-E16.5 spinal cords for β-gal and Sox2. Arrowheads point out the most distal cells. (J) Relative distance of front runner β-gal$^+$,Sox2$^+$ nuclei (top 10%) from the vz border. (K-P) Developing Dbx1-derived astroglial cells are morphologically heterogeneous. Mosaic tomato labeling was induced by low Tam doses at E11.75 in *Nestin:CreER;CAG:LSL-tdTomato* and analyzed at E15.5 and E16.5. (K-M′) E15.5 spinal section stained for Tomato and β-gal. Magnification of p0 domain with a β-gal$^+$,Tomato$^+$ cell in the vz (L,L′, arrowhead) and two cells with dissimilar morphologies in the mantle zone (M,M′, arrowheads). (N,O) Representative images of cell morphologies at E16.5. Multipolar cells accounted for 23% (*n*=90/399), and the remaining 77% were cells with unipolar or bipolar morphology (*n*=309/399). (P) Multipolar cells were observed mainly in the pGM, whereas uni/bipolar β-gal cells were in more lateral regions, mostly in dGM and WM. Scale bars: 50 µm (A,E,G-I,K); 20 µm (B-D,E′,E″,F,L-M′); 10 µm (N,O). Values are mean+s.d.

vA0 precursors intensively proliferate distal to the vz

Quantification of β-gal$^+$ cells in the parenchyma revealed a continued increase from E13.5 to E18.5 (Fig. 4A). This rise was accompanied by attrition of the p0 vz, which at E16.5 contained few remaining cells (Fig. 4B). To determine the expansion of the vA0 population during the migratory journey, we assessed their proliferation with bromodeoxyuridine (BrdU) labeling. At E13.5, about 7% of β-gal$^+$ vz cells incorporated BrdU (Fig. 4C). Later, the number of β-gal$^+$,BrdU$^+$ cells drastically increased in the mantle zone reaching a proliferation peak at E16.5 (24.1±8.5%; Fig. 4C,D). These stages with high division rates in the mantle coincided with the largest expansion of vA0 cells (Fig. 4A). Proliferation at E16.5 was not restricted to any preferential morphology, with multipolar and uni/bipolar cells incorporating BrdU (~23-25%; Fig. S3I-K). Cell divisions were largely biased to distal positions, as 90% of BrdU-labeled cells were in the dGM and WM (Fig. 4E-G). Further analysis revealed that proliferation persisted at E18.5 although significantly decreased (E18.5: 7.8±2.1%; Fig. 4C) and β-gal$^+$,

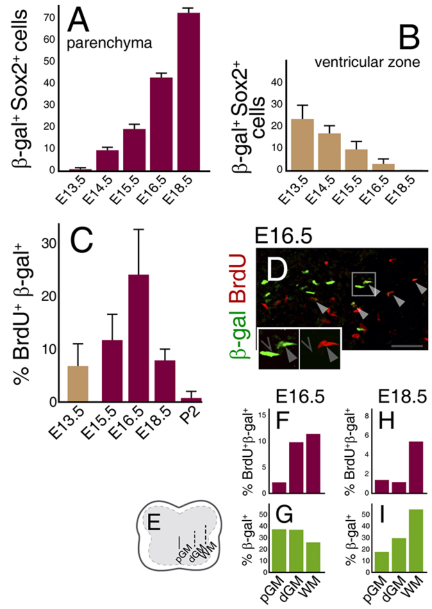

Fig. 4. vA0 cells extensively divide during migration. (A,B) Quantification of β-gal⁺,Sox2⁺ cells in the E13.5-E18.5 spinal cord mantle zone (A) or within the vz (B); (>20 sections, at least three embryos). (C-I) The β-gal⁺ population expands outside the vz. (C) Percentage of β-gal⁺ cells that incorporated BrdU at different stages (at least ten sections, two to three embryos). (D) E16.5 spinal cord showing colocalization of β-gal and BrdU. Arrowheads indicate double-labeled cells, carets indicate β-gal⁺,BrdU⁻ cells. Insets show enlarged views of the boxed region. (E-I) Proportion of β-gal⁺,BrdU⁺ cells in medial-lateral regions (F,H) and distribution of β-gal⁺ cells (G,I) at E16.5 and E18.5 (n=377 and 615 cells, respectively). E shows a diagram of the regions examined. Scale bar: 50 µm. Data are expressed as mean+s.d. See also Fig. S3.

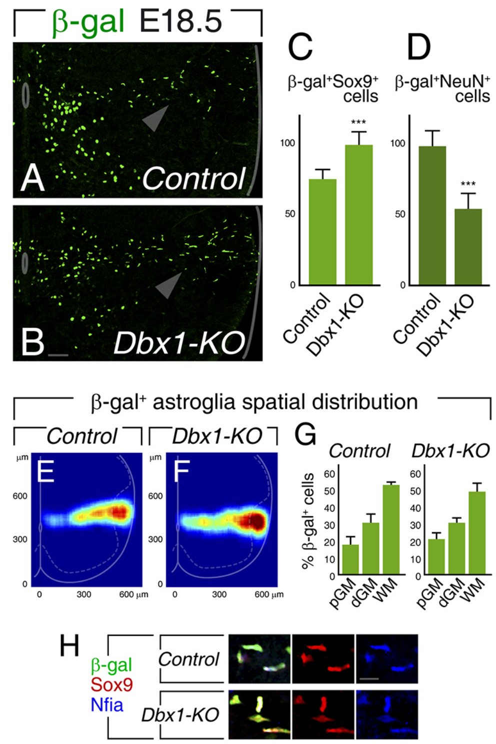

Fig. 5. Dbx1 controls the size of the astroglial vA0 population. (A-D) *Dbx1* mutants have increased p0-derived astrocytic cells at the expense of V0 neurons. (A,B) E18.5 control and *Dbx1-KO* spinal cord cross-sections. Arrowheads point to the intermediate spinal cord. (C,D) Quantification of astroglial β-gal⁺,Sox9⁺ (C) and neuronal β-gal⁺,NeuN⁺ (D) cells per section; 35±13% increment and 44±9% decline, respectively (n=22 sections from three embryos; ***P< 0.001, Mann–Whitney test). (E,F) Spatial maps of β-gal⁺,Sox9⁺ cells in control and *Dbx1* mutants made from 650 and 895 β-gal⁺ cells, respectively. (G) The distribution of cells in the medial-lateral axis is similar between genotypes (non-significant, Mann–Whitney test). (H) β-Gal⁺ cells in control and *Dbx1*$^{-/-}$ spinal cords are co-labeled with the glial markers Sox2 and Nfia. Scale bars: 50 µm (A,B); 10 µm (H). Values are mean+s.d. See also Fig. S4.

BrdU⁺ cells were mostly in the WM (>80%; Fig. 4H,I). Postnatally, BrdU⁺ cells were very reduced (Fig. 4C). Overall, these experiments show that vz Dbx1⁺ radial glia produce heterogeneous intermediate astrocyte precursors, which intensively amplify outside the germinal zone in distal regions of the spinal cord to shape the postnatal vA0 population.

Dbx1 regulates the development of the vA0 population

Dbx1 has important functions in the specification of V0 neurons in the spinal cord and hindbrain (Pierani et al., 2001; Lanuza et al., 2004; Zagoraiou et al., 2009; Bouvier et al., 2010). To evaluate the role of Dbx1 in differentiation of the late p0 progeny, we produced *Dbx1* mutants containing the *Dbx1*^{lacZ} reporter/null allele to allow cell tracing. We first obtained E18.5 *Dbx1* heterozygotes and mutants and found a significant expansion of β-gal⁺,Sox9⁺ cell number in the *Dbx1-KO* (*Dbx1*$^{-/-}$) spinal cord (Fig. 5A-C; 35±13% increase). To characterize the mutant vA0 population further, we studied its spatial distribution and saw that *Dbx1*$^{-/-}$ β-gal⁺ cells were confined to a region similar to control heterozygotes (Fig. 5A, B,E,F, Fig. S4A). In addition, their radial positions from the midline to the lateral funiculus were unchanged (Fig. 5E-G). We spotted a slight ventral angular shift (Fig. S4A,B), which is likely to be a consequence of lamina VIII reduction in *Dbx1-KO* animals. As in controls, β-gal⁺ cells in *Dbx1-KO* samples expressed Sox2, Sox9 and Nfia (Fig. 5H, Fig. S4C-E) and were Olig2 and NeuN negative (Fig. S4C,E). Hence, in the absence of Dbx1, late-born p0 cells still possess astrocytic character.

Interestingly, we noticed that the increment of glial β-gal⁺ cells in *Dbx1-KO* animals was accompanied by a decrease in the number of β-gal⁺ neurons in the ventromedial cord (Fig. 5A-D). We also observed this phenotype in the hindbrain, where Dbx1 mutants had an increased number of β-gal⁺,Sox9⁺ cells, but neurons were reduced (Fig. S4F-J).

In summary, *Dbx1* mutant spinal cord and hindbrain have an enlarged vA0 population and a diminished number of neurons produced by the same ventricular domain. These results demonstrate that, in addition to the specification of V0 interneurons, Dbx1 controls the differentiation of p0-derived astroglial cells.

Dbx1 defines the prospective astrocytic progenitor pool

The observation that vA0 astrocytes are increased in *Dbx1*$^{-/-}$ mice prompted us to define when and how Dbx1 acts on astrogliogenesis. Several possibilities could explain this phenotype in *Dbx1-KO*: developing vA0 s amplify at higher rates, glial cells are prematurely born, or ventricular p0 precursors are already increased in mutants at the neurogenesis-gliogenesis switch.

First, we analyzed the expression of *Dbx1* throughout development and confirmed its expression in the vz and absence in the mantle zone (Fig. 6A-E, Fig. S5A-A″), suggesting that Dbx1 acts in progenitors. Second, we quantified the number of β-gal⁺, Sox9⁺ glial cells in the mantle zone of control and mutant mice from E13.5 to E18.5. The vA0 population was higher in *Dbx1*$^{-/-}$, its increase being already statistically significant at E14.5 (Fig. 6F). To define whether the increment rate of developing vA0 during this

Development (2022) 149, dev200750. doi:10.1242/dev.200750

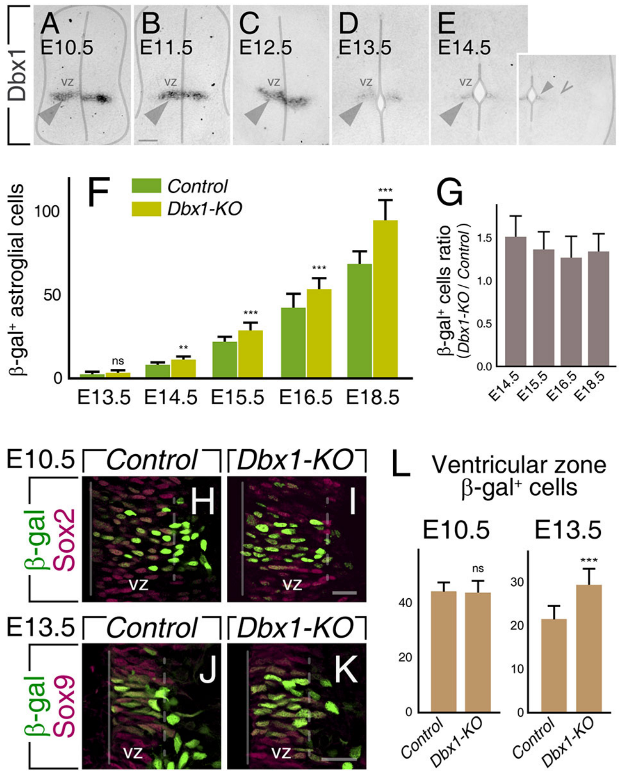

Fig. 6. Dbx1 delineates the p0 progenitor pool and vA0 astroglial population. (A-E) *Dbx1* is expressed at the p0 vz (arrowheads) and absent in the mantle zone (caret). (F) Quantification of β-gal$^+$,Sox9$^+$ cells outside the vz in control and *Dbx1*-null E13.5-E18.5 cords (at least ten sections from two to three embryos of each genotype/stage; $^{**}P<0.01$,$^{***}P<0.001$, Mann–Whitney test). (G) Ratio of β-gal$^+$ glial cells in *Dbx1-KO* to control (non-significant, Kruskal–Wallis with post-hoc Dunn's test). (H-L) Late p0 vz progenitors are increased in *Dbx1* mutants. (H-K) Transverse sections of E10.5 and E13.5 embryos stained against β-gal and Sox2 or Sox9. Dashed line delineates the vz. (L) Quantification of β-gal$^+$,Sox2/9$^+$ cells in the vz. No differences were seen near the onset of the neurogenic stage (E10.5), whereas *Dbx1-KO* have increased β-gal$^+$ progenitors at E13.5 (38±23% increment; 10-16 sections, two to three embryos each; ns, non-significant; $^{***}P<0.001$, Mann–Whitney test). Scale bars: 30 µm (A-E); 20 µm (H-K). Data are expressed as mean+s.d. See also Fig. S5.

period is different in *Dbx1*$^{-/-}$, we determined the ratio of β-gal$^+$ cells in *Dbx1-KO* over control samples. This number was constant at all stages, indicating proportional increases in controls and mutants (Fig. 6G; global average 1.36±0.08). Lastly, we did not observe differences in β-gal$^+$,Sox9$^+$ cells outside the vz at E13.5 (Fig. 6F), ruling out premature gliogenesis onset in *Dbx1-KO*.

Altogether, these results suggest that Dbx1 limits the vA0 population by acting early, before p0 start astrocytic production. To test this possibility, we analyzed the vz at the neuron-glia transition. In *Dbx1* mutants, we found that β-gal$^+$,Sox9$^+$ numbers were significantly increased within the E13.5 p0 domain (Fig. 6J-L), indicating that the expansion seen in the mutant relates to an enlarged late progenitor pool with astroglial potential. To determine when the p0 domain increases in *Dbx1*$^{-/-}$ animals, we analyzed the E10.5 vz, and found that p0 neuroepithelial progenitor numbers were similar in *Dbx1-KO* and control samples (Fig. 6H,I,L). This indicates that the increase in p0-domain progenitors takes place during the neurogenic phase before gliogenesis begins. Moreover, the proportional increase rate of vA0 cells and the absence of premature vz exit in *Dbx1-KO* eliminates the possibility of Dbx1 controlling vA0 population during the gliogenic phase. We propose that Dbx1-dependent modulation of astrogenesis is a consequence of Dbx1 acting during the neurogenic period, establishing the size of the late progenitor pool with the potential to produce vA0 cells.

Dbx1 controls astroglial development by directing Notch ligand expression

Changes in neuron-astrocyte balance in *Dbx1* mutants are reminiscent of phenotypes with altered Notch signaling (Louvi and Artavanis-Tsakonas, 2006; Pierfelice et al., 2011; Freeman, 2010). To explore the relationship between Dbx1 and Notch signaling in determining late p0 progenitor number and astroglial progeny, we evaluated key components of the Notch-Delta pathway. Previous studies have shown that specific ligand-receptor pairs distinctly activate Notch signaling and that post-translational modifications of Notch are crucial in ligand activation (Hicks et al., 2000; Yang et al., 2005; Kakuda and Haltiwanger, 2017). The Notch ligands Dll1 and Jag1 display a striped expression pattern in DV neural tube domains (Lindsell et al., 1996; Myat et al., 1996; Marklund et al., 2010; Ramos et al., 2010). We observed that the p0 domain expresses *Dll1*, which was also present in other ventricular territories (Fig. 7A-C,E). Likewise, *Jag1* was restricted to the p1 and pd6 domains, bordering dorsally and ventrally the *Dbx1*$^+$ vz (Fig. 7A,B,D,F). The gene encoding the glycosyltransferase Lfng, known to modify Notch receptor properties (Hicks et al., 2000; Yang et al., 2005; Kakuda and Haltiwanger, 2017), showed an expression largely similar to that of *Dll1* (Fig. 7E,G).

The analysis of Notch ligand patterning in E10.5 *Dbx1-KO* mice showed that the p0 region switched to *Jag1* positive, and *Dll1* and *Lfng* negative (Fig. 7H-J). The altered pattern in *Dbx1* mutants was seen throughout the neurogenic period (E11.5 and E12.5; Fig. S5B-K), whereas Notch1/2 receptor gene expression in mutants was unaltered (Fig. S5L-O). *Dll3*, present in cells fated for terminal neuronal differentiation at the vz-mantle transition (Dunwoodie et al., 1997), was reduced in *Dbx1-KO* mice, likely reflecting diminished p0 neurogenesis (Fig. S5P,Q).

These results suggest that in *Dbx1-KO* Jag1, expressed in committed neuronal precursors, is more efficient at activating Notch signaling in neighboring progenitors than Dll1 (Hicks et al., 2000). Consistent with this, we found that *Dbx1* mutants have fewer Neurog2$^+$ neuron-committed cells in their p0 domain (Fig. 7K-M), and a reduced population of β-gal$^+$ neurons (Fig. 7N-P). As shown above, the reduction in the pace of neurogenesis in *Dbx1* mutants is accompanied by an increase in undifferentiated progenitors at the end of the neurogenic period.

vA0 development is dependent on early Notch signaling

To assess how Notch signaling is involved in the regulation of V0 and vA0 fates, we first generated presenilin1 (*Psen1*) mutants, in which Notch activation is impaired. Presenilin is the catalytic component of the γ-secretase complex, which is responsible for processing several membrane substrates, including Notch receptors after ligand activation (Selkoe and Kopan, 2003; Parks and Curtis, 2007). At E18.5, the number of vA0 cells in *Psen1*$^{-/-}$ spinal cords was severely reduced (Fig. 8A-C, dotted boxes), whereas V0 neurons were increased (Fig. 8A,B,D), providing evidence that perturbations in the Notch pathway result in profound alterations in p0 cell identities.

To define when Notch signaling is relevant in vA0 development, we pharmacologically perturbed Notch processing using the γ-secretase inhibitor Ly411575. Ly411575 was applied at E10.5 (neurogenic phase), E13.5 (neurogenic-gliogenic transition) or E15.5 (astrocytic migration/expansion period). Ly411575

Development (2022) 149, dev200750. doi:10.1242/dev.200750

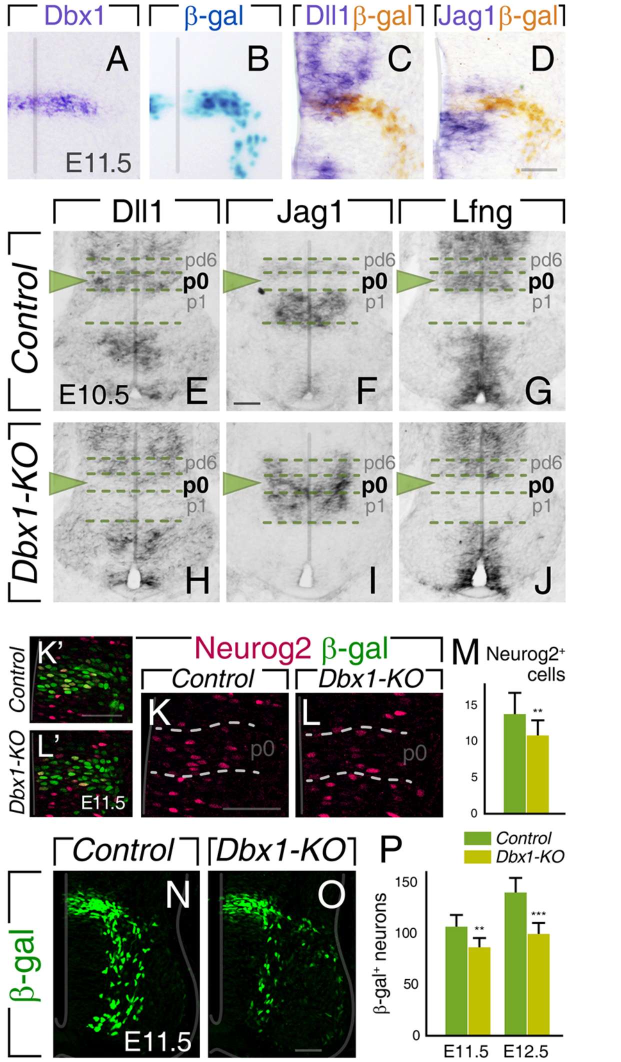

Fig. 7. Dbx1 controls the expression of Notch regulatory proteins and neurogenesis in p0 domain. (A-D) Cells within the p0 domain express *Dll1* but not *Jag1*. E11.5 neural tube hybridized for *Dbx1*, developed for β-gal and hybridized for *Dll1* or *Jag1* with β-gal immunostaining. (E-J) Dbx1 regulates Notch ligand expression. *In situ* hybridization at E10.5 showing that *Dll1* and *Lnfg* in the p0 region are replaced by *Jag1* expression in *Dbx1* mutants. Arrowheads indicate the p0 domain. (K-P) Neurogenesis from p0 progenitors is reduced in *Dbx1-KO*. (K-M) Immunostaining of control and *Dbx1-KO* E11.5 spinal cord against Neurog2 (K-L′) and the associated quantification (M) (**P<0.01, Mann–Whitney test). (N-P) β-Gal$^+$ mantle zone cells in *Dbx1* mutants are diminished at E11.5 and E12.5 (**P<0.01, ***P<0.001, Mann–Whitney test). Data are expressed as mean+s.d. Dashed lines mark the boundaries between vz progenitor domains. Scale bars: 50 µm. See also Fig. S5.

administration at E13.5 or E15.5 did not result in changes in vA0 number (Fig. 8E). However, when embryos were treated at E10.5, we found a notable decrease in vA0 cells at E16.5, similar to observations in *Psen1-KO* (Fig. 8E-H). These results confirm that perturbations in Notch signaling in an early developmental window highly influence the specification of p0 astrocyte precursors. To verify that Notch inhibition at E10.5 also modulates neuronal differentiation, we analyzed the V0 marker Evx1 at E11.5. As expected, there was an increase in V0 interneurons, with Evx1-expressing neurons ectopically immersed in the vz, reflecting premature differentiation (Fig. 8I-K). Altogether, these experiments demonstrate that early Notch–mediated cell–cell interactions in the

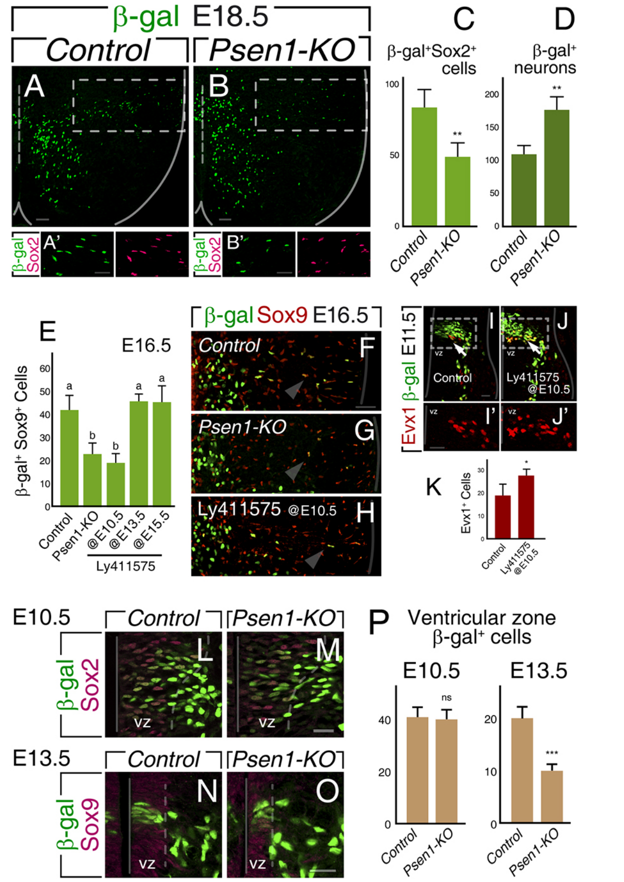

Fig. 8. Notch signaling balances glial-neuronal p0 fate. (A-D) The vA0 population is decreased after Notch signaling abrogation. E18.5 *Psen1$^{+/+}$* (control) and *Psen1-KO* stained for β-gal (A-B′) and Sox2 (A′,B′). A′ and B′ show enlarged views of the boxed areas above. Dashed vertical lines indicate the midline. (C,D) Number of β-gal$^+$,Sox2$^+$ (C) and β-gal$^+$,Sox2$^-$ (D, neurons) cells per section; 40±7% reduction and 63±19% increment, respectively (n=12 sections from three embryos; **P< 0.01, Mann–Whitney test). (E-K) Early Notch signaling inhibition affects vA0 differentiation. (E-H) Number of β-gal$^+$,Sox9$^+$ cells per section at E16.5 after treating with vehicle (control) or Ly411575 at E10.5, E13.5 or E15.5 (at least ten sections, two to three embryos). Letters indicate significant differences between groups (P<0.01, Kruskal–Wallis with post-hoc Dunn's test). Arrowheads indicate β-gal$^+$, Sox9$^+$ cells. (I-K) Early pharmacological Notch signaling inhibition increases neurogenesis. Evx1 staining in E11.5 embryos treated with vehicle or Ly411575 at E10.5 (I-J′) and the associated quantification (K) (*P<0.05, Mann–Whitney test; at least ten sections, two embryos each). Arrows in I,J indicate Evx1$^+$ neurons. I′ and J′ show enlarged views of the boxed areas above. (L-P) Late p0 progenitors are diminished in *Psen1-KO*. (L-O) Cross-sections of the p0 ventricular domain of control and *Psen1-KO* spinal cord at E10.5 and E13.5 stained for β-gal and Sox2 or Sox9. (P) Quantification of β-gal$^+$,Sox2/9$^+$ cells in control and *Psen1-KO* vz at E10.5 and E13.5. No difference was found at E10.5, while the p0 cells were significantly decreased at E13.5 (49±6% reduction, 12 sections, two to three embryos each; ns, non-significant; ***P<0.001, Mann–Whitney test). Dashed lines mark vz limits. Scale bars: 50 µm (A,B,F-H); 30 µm (A′,B′); 20 µm (I-J′,L-O). Values are mean+s.d.

p0 domain define not only neuron production, but also late glial development.

Finally, we examined how abrogation of Notch signaling impacts the p0 pool available for glial differentiation. In *Psen1* mutants, we found a drastic decrease in the number of p0 vz cells at E13.5 (Fig. 8N-P). *Psen1-KO* mice had normal p0 numbers at E10.5 (Fig. 8L,M,P), implying that the differences seen at E13.5 are acquired during the neurogenic phase. These results show that Notch signaling

Development (2022) 149, dev200750. doi:10.1242/dev.200750

perturbations generate increased and premature neuron production, leading to a reduced late p0 progenitor pool at the beginning of the gliogenic phase. Together with data presented above (Fig. 5), these results demonstrate that Dbx1 and Notch modulate p0 progenitor behavior during the neurogenic period, controlling the balance between neuron production and preservation of undifferentiated vz cells with the potential of subsequently giving rise to vA0 astrocytes.

DISCUSSION

This study shows that neural progenitors of the vz p0 domain expressing Dbx1 generate astroglial precursors that cover a specific region of the mouse spinal cord following a stereotyped radial migration (Fig. 9). The Dbx1-derived glial population is composed of GM protoplasmic, WM fibrous and WM radial astrocytes that distinctively express reelin and Kcnmb4. Although it is known that Dbx1 plays a fundamental role in V0 neuron identity (Pierani et al., 2001; Lanuza et al., 2004; Zagoraiou et al., 2009), here we demonstrate that it also controls astrocyte number through Notch signaling modulation.

The precise allocation of vA0 cells and the formation of astroglial maps

We demonstrate that astrocytic cells derived from late p0 progenitors display an invariant positional arrangement in the mouse spinal cord. Mirroring the DV ventricular origin, vA0 population precisely occupies the entire intermediate portion of the spinal cord from the midline to the lateral funiculus, spatial restriction that is retained postnatally. Together with previous studies, the results presented here emphasize positional identity as a central developmental principle in the production of diverse glial populations of the spinal cord (Hochstim et al., 2008; Tsai et al., 2012; Vue et al., 2014). Like neuronal subtype specification, astrocyte diversification is highly influenced by the transcriptional code patterning DV progenitors (Hochstim et al., 2008; Muroyama et al., 2005; Vue et al., 2014; Zhao et al., 2014).

Interestingly, in line with descriptions in the mouse, a recent analysis of the midgestation human spinal cord have shown astrocytes with specialized DV transcriptional programs, and gene expression signatures map also onto distinct anatomical domains (Andersen et al., 2021 preprint). In addition, studies in the *Drosophila* larval ventral nerve cord have shown that individual astrocytes are allocated to consistent positions with their arbors covering stereotyped territories of the neuropil (Peco et al., 2016). This developmental phenomenon, conserved in humans, mice and flies, suggests that astrocyte origin and final location is not incidental and that spatially restricted groups of astrocytes are fitted to play specific roles in local neuronal circuits and microcircuits. In support of the connection between allocation and function, ventral horn astrocytes have been shown to play dedicated functions preserving motoneuron and sensorimotor circuit integrity (Molofsky et al., 2014; Kelley et al., 2018).

We found that reelin and Kcnmb4 are WM vA0 molecular markers. Reelin was previously proposed to identify vA1 and vA2 WM astrocytes (Hochstim et al., 2008; Zhao et al., 2014). Here, we show that reelin is also present in Dbx1-derived astrocytes appearing after vA0s have left the germinal zone. Its induction is likely dependent on Pax6, which persists in vA0 precursors and has the capacity to promote reelin expression (Hochstim et al., 2008). Otherwise, Kcnmb4, encoding the β4 subunit of BK channels, is already present in p0 ventricular precursors before their migration. It is intriguing to know the role of Kcnmb4 in WM vA0 astrocytes. In the brain, BK channels are located at astrocyte endfeet wrapping parenchymal vessels and pial arterioles (Contet et al., 2016; Filosa et al., 2006; Girouard et al., 2010). These channels, properties of which are adjusted by the β4 auxiliary subunit, are activated by neuronal stimulation to modulate smooth muscle contraction-relaxation, linking neuronal activity with local blood flow.

Our experiments show that the late Dbx1-expressing progeny is composed exclusively of astroglial cells. This observation clashes with a previous study identifying oligodendrocytes being derived from the DV intermediate vz region (Fogarty et al., 2005). This contradiction might result from the mapping strategies used; in *Dbx1*^{lacZ} mice, β-gal restricts to p0 cells, whereas *Dbx1:Cre* transgene expression includes the dp5-dp6 domains (Fogarty et al., 2005), which are a source of dorsal spinal oligodendrocytes (Cai et al., 2005; Vallstedt et al., 2005).

vA0 astrocytes are morphologically heterogeneous

Sparse labeling of Dbx1-derived glia at perinatal stages revealed their morphological heterogeneity. The vA0 population includes cells with features of the two classic astrocytic subtypes, protoplasmic and fibrous (Oberheim et al., 2012; Peters et al., 1991; Tabata, 2015) (Fig. 9B,C). Protoplasmic astrocytes have complex structures with numerous and highly branched processes and are intermingled with neurons in the intermediate spinal GM. In contrast, vA0 cells with fibrous-like appearance are less complex with straight processes oriented longitudinally with axon fibers in the WM and express high levels of Gfap. The third vA0 morphological subtype is composed of radially oriented cells in the WM, also expressing Gfap and displaying conspicuous processes contacting the pia (Fig. 9B,C).

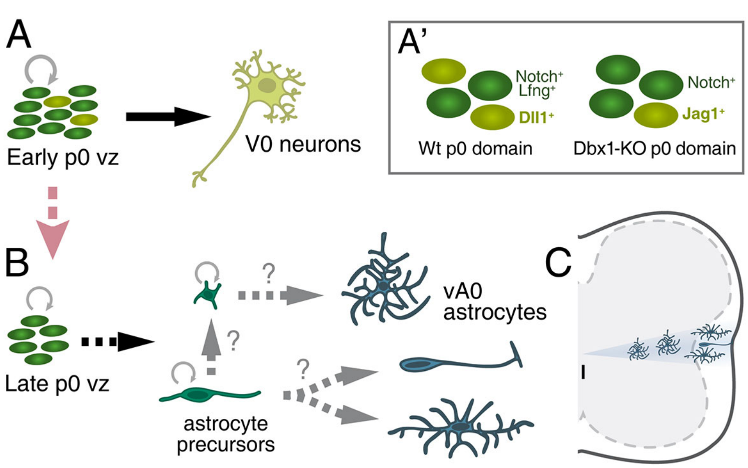

Fig. 9. Dbx1 progenitors produce a heterogeneous population of spinal astrocytes. (A) Schematic of the E10-E12 p0 domain and V0 interneurons. (A′) In the *Dbx1-KO* spinal cord, neuronal precursors express Jag1 instead of Dll1, resulting in expansion of the astrocyte progenitor pool. (B,C) During the gliogenic phase, the late p0 domain produces astrocytic precursors that migrate radially to colonize a specific region of the postnatal spinal cord. The vA0 population comprises GM protoplasmic, WM fibrous and WM radial astrocytes. GM is represented by gray shading bound by a dashed line. Blue shading represents the territory occupied by vA0 cells.

Development (2022) 149, dev200750. doi:10.1242/dev.200750

Cells with these characteristics have been recognized as important participants in the formation and maintenance of the glia limitans, which covers the spinal cord surface (Liuzzi and Miller, 1987; Liu et al., 2013). In the adult, these radially arrayed WM cells at the pial boundary have been shown to become activated after autoimmune demyelination or contusive spinal cord injury (Petit et al., 2011).

Morphological astrocyte diversity appears to be a general characteristic of regionally related astrocytic progenies. Several studies have shown that other astrocyte groups dorsal and ventral to the vA0 population also contain both GM and WM astrocytes (Tsai et al., 2012; Hochstim et al., 2008; Vue et al., 2014; Fogarty et al., 2005; Zhao et al., 2014). It remains to be established how GM and WM astrocytes are specified. Interestingly, in the dorsal spinal cord, Ascl1-expressing glial progenitors are restricted to become either GM or WM astrocytes or oligodendrocytes (Vue et al., 2014). Similarly, in the developing cortex, different astrocytic classes appear to emerge from separate clones (García-Marqués and López-Mascaraque, 2013; Shen et al., 2021). Conversely, other clonal analyses in the cortex have shown extensive morphological and location variability in astrocytes within clones (Clavreul et al., 2019), suggesting that cues from neighboring neurons influence astrocyte specialization (Farmer et al., 2016). Further studies will be required to determine whether individual p0 radial glial cells produce different astrocytic subtypes by symmetric or asymmetric division and how intrinsic and extrinsic cues act to sculpt vA0 astrocyte heterogeneity.

Radial migration and proliferation in the parenchyma delineate vA0 spatial distribution

Dbx1-derived astrocyte precursors begin exiting the p0 vz domain around E13.5, and their number progressively rises until birth. Our experiments indicate that the vA0 population depends primarily on cells emanating from the vz, and later on their proliferation in the parenchyma (Fig. 9B). From E15.5 to E18.5, when the vz contribution is minor, the vA0 population expands three- to fourfold. Such intense proliferation outside the germinal zone is a defining characteristic of astrocytic development, and has been shown in the cerebral cortex and in other regions of the spinal cord (Barry and McDermott, 2005; Tien et al., 2012; McMahon and McDermott, 2001; Ge et al., 2012). BrdU labeling shows that proliferation mainly takes place at distal-lateral positions, in the dGM and WM. Because more lateral territories covered by vA0s are larger than regions closer to the midline, they presumably require more cells. This distal expansion probably relies on the BRAF-MAPK pathway activated by local mitogens released from the basal lamina or secreted by neighboring neurons (Tien et al., 2012).

Direct observation of brain and spinal cord acute slices has shown that cells with a leading process attached to the pia travel through the tissue by continuous shortenings of their cellular extension (Nadarajah et al., 2001; Pakan and McDermott, 2014). The morphology of radial glial progenitors, i.e. long cellular extensions spanning the thickness of the spinal cord, from their soma in the vz to the basal lamina, allows the vA0 migratory route toward the pia to be anticipated (McMahon and McDermott, 2002; Barry and McDermott, 2005). Dbx1-derived astroglial precursors progressively colonize lateral areas of the spinal cord following strictly radial movements. In this path from the vz to the parenchyma, we found that ∼75% of vA0 precursors in the mantle are highly polarized and possess a prolonged extension toward the pia. This cell morphology and the gradual lateral displacement of nuclei suggest vA0 precursors mainly migrate by translocating their soma. Further studies are needed to establish whether multipolar precursors, which account for ∼25% of cells at E15-E16, are directly produced from the vz progenitors or if they arise through transformation of uni/bipolar precursors sowing the entire medial-lateral axis with vA0 cells (Fig. 9B).

Dbx1 regulates Notch ligand expression and neuron-astrocyte fate balance

The Notch signaling pathway plays a fundamental role in neuronal and glial development and undifferentiated pool preservation (Louvi and Artavanis-Tsakonas, 2006; Pierfelice et al., 2011). High activation of Notch receptors in neural progenitors limits their neurogenic differentiation, while increasing glial commitment (Henrique et al., 1995; Chitnis, 1995; Gaiano et al., 2000; Park and Appel, 2003; Kong et al., 2015). Conversely, loss of key factors, such as Notch receptors or Rbpj triggers early increased neurogenesis and progenitor depletion (de la Pompa et al., 1997; Lütolf et al., 2002; Taylor et al., 2007; Kong et al., 2015). In addition, Notch signaling is known to regulate the transcription factors Nfia and Sox9, which are key players in glial commitment and gliogenesis onset (Deneen et al., 2006; Stolt et al., 2003; Kang et al., 2012). Notch activation in neural progenitors induces Nfia (Namihira et al., 2009) and helps to maintain Sox9 expression (Taylor et al., 2007).

In the neural tube, the Notch ligands Dll1 and Jag1 are expressed in discrete complementary DV territories, which define different quantitative levels of Notch signaling and neuron production rates in specific domains (Lindsell et al., 1996; Myat et al., 1996; Marklund et al., 2010; Ramos et al., 2010). We show that in the absence of Dbx1 the p0 domain switches from Dll1 to Jag1 expression (Fig. 9A′), which is in line with patterning genes controlling the DV Notch ligand distribution (Skaggs et al., 2011; Marklund et al., 2010). In addition, *Dbx1-KO* progenitors lack the glycosyltranserase Lfng (Fig. 9A′), which is known to suppress the ability of Jag1 to activate the pathway (Hicks et al., 2000; Yang et al., 2005; Kakuda and Haltiwanger, 2017). Thus, combined changes in both Notch-responding cells ($Lfng^+$ to $Lfng^-$) and ligand-presenting precursors ($Dll1^+$ to $Jag1^+$) contribute to enhance Notch signaling within the *Dbx1* mutant p0 domain, attenuating neuron differentiation and increasing glial production.

The absence of Dbx1 could also result in astrocytic subgroup identity changes, with vA0 cells adopting the molecular properties of vA1 or dA6 subpopulations. This alternative is in line with the transcriptional code controlling not only neuronal specification, but also the molecular identity of ventral spinal cord astrocyte subsets (Hochstim et al., 2008; Zhao et al., 2014), and should be studied upon identification of selective markers.

Our results highlight a role for Dbx1 in adjusting the size of p0-derived neuronal and glial populations. Strict control of neurogenesis is necessary not only to generate the appropriate number of V0 neurons, but also to preserve undifferentiated progenitors and their subsequent differentiation into vA0 cells. Dbx1-dependent expression of key Notch factors, together with the phenotypes of *Dbx1* mutants and after Notch manipulations, and the temporal coincidence of the essential actions of Dbx1 and Notch strongly support a mechanistic connection in the regulation of neuron-astrocyte cell fate balance.

MATERIALS AND METHODS

Animals

All experiments involving animals were conducted according to the protocols approved by the Institutional Animal Care and Use Committee (IACUC) of the Fundación Instituto Leloir. Genotyping of $Dbx1^{lacZ}$ (Pierani et al., 2001), $Glast^{CreER}$ (Mori et al., 2006), *Nestin:CreER* (Carlen et al., 2006), *Psen1* (Shen et al., 1997) and *Ai14 tdTomato* conditional reporter (Madisen et al., 2010) mice were performed by PCR using allele-specific primers for each strain.

Timed pregnancies were determined by detection of vaginal plug and midday was designated E0.5. Maximum induction of Cre activity in $Glast^{CreER}$ mice was achieved with intraperitoneal injection of 150 mg/kg body weight of tamoxifen in corn oil (Tam; Sigma-Aldrich) administered to pregnant females. Mosaic labeling in transgenic *Nestin:CreER* mice was performed with Tam at a dose of 37.5 mg/kg body weight injected at E11.75.

Embryos were dissected in PBS buffer. After decapitation, embryos were pinned on Sylgard plates, eviscerated and fixed for 1 h in 4% paraformaldehyde (PFA) in PBS followed by cryoprotection in 20% sucrose (overnight, 4°C) prior to embedding in Cryoplast (Biopack). Stage-matched littermates of the desired genotypes were aligned and embedded together to ensure identical processing conditions. Tissue was cryosectioned at 30 µm thickness, except in mosaic labeling experiments (45 µm) (Leica 3050S, Leica Biosystems).

For BrdU labeling, pregnant females or pups were injected intraperitoneally with a single dose of BrdU (50 mg/kg body weight) and tissue was collected 3 h later. The γ-secretase inhibitor Ly411575 (Hyde et al., 2006) was administered subcutaneously to timed-pregnant dams at 5 mg/kg body weight (at E10.5, E13.5 and E15.5 stages). Animals treated with vehicle (dimethyl sulfoxide in corn oil) served as controls in these experiments. The effectiveness of Ly411575 was controlled by appearance of tail shortening (when applied at E10.5) or hemorrhages in limbs and head (when injected at E13.5 or E15.5).

Immunohistochemistry and *in situ* hybridization

Antibody staining was performed essentially as previously described (Di Bella et al., 2019). Briefly, sections were treated with blocking solution [5% HI-serum (Natocor), 0.1% Triton X-100 in PBS] for 1 h and incubated with primary antibodies in blocking solution overnight at 4°C. Antibodies used were: anti-Nkx2-2 [74.5A5, Developmental Studies Hybridoma Bank (DSHB) 1:20], anti-Nkx6-1 (F55A10, DSHB, 1:20), anti-Pax6 (#pax6, DSHB, 1:20), anti-β-gal (55976, Cappel, now MP Biomedicals, 1:1000; and from Martyn Goulding, Salk Institute, CA, USA, 1:1000), anti-Sox2 (SC17320, Santa Cruz Biotechnology, 1:300; or MAB2018, R&D Systems, 1:50), anti-Sox9 (AF3075, R&D Systems, 1:200), anti-Nfia (39397, Active Motif, 1:1000), anti-Dbx1 (from Tom Jessell, Columbia University, NY, USA; 1:250), anti-NeuN (A60, Chemicon, 1:500), anti-Olig2 (AB9610, Chemicon, 1:1000), anti-Gfap (from Fred Gage, Salk Institute, 1:2500), anti-Evx1 and anti-Pax3 (from Martyn Goulding, Salk Institute; 1:1000 and 1:400), anti-nestin (from Fred Gage, Salk Institute, 1:500), anti-BrdU (MCA2060T, AbD Serotec, now Bio-Rad, 1:250), anti-Neurog2 (Sc-19233, Santa Cruz Biotechnology, 1:500), anti-reelin (ab78540, Abcam, 1:500), anti-Jag1 (Sc-6011, Santa Cruz Biotechnology, 1:200) and anti-dsRed (632496, Clontech, 1:300).

For detection, Cy-labeled species-specific secondary antibodies (Jackson ImmunoResearch, 715-225-151, 715-165-151, 715-175-151, 711-225-152, 711-165-152, 711-175-152, 712-225-153, 712-165-153, 712-175-153, 706-225-148, 706-165-148, 706-175-148, 703-065-155, 705-065-147) were incubated for 3-4 h at room temperature. For BrdU staining, acidic antigen retrieval was performed prior to immunodetection. Sections were mounted with PVA-DABCO (P8136, D2522, Sigma-Aldrich), or dehydrated in an ethanol/xylene series and mounted with DPX (06522, Sigma-Aldrich).

Non-radioactive *in situ* hybridization was performed as previously described (Carcagno et al., 2014). Sections were fixed with 4% PFA and washed with PBS-DEPC. Tissue was treated with proteinase K (3 µg/ml, 3 min), followed by 4% PFA for 10 min and three PBS washes, 3 min each, at room temperature. Slides were incubated in triethanolamine-acetic anhydrate, pH 8.0, for 10 min and permeabilized with 1% Triton X-100 for 30 min. Sections were incubated for 2 h with hybridization solution (50% formamide, 5× SSC, 5× Denhardt's solution, 250 µg/ml yeast tRNA). Digoxigenin (DIG)-labeled RNA probes were generated by *in vitro* transcription using linearized plasmids or PCR-amplified products as templates, with T7, T3 or sp6 RNA polymerases (Promega), DIG-UTP (Roche), rNTPs (Promega). The cDNA templates used were Dbx1 and Dll1 (from Martyn Goulding, Salk Institute), Notch1 and Notch2 (from Geraldine Weinmaster, UCLA, CA, USA), Jag1, Dll3, Lfng and Kcnmb4 (this study). Dig-labeled probes were diluted in hybridization solution, denatured and incubated for 14 h at 68°C. Slides were washed three times, 45 min each wash, at 68°C with 1× SSC, 50% formamide. For detection, sections were blocked with 10% HI-serum for 2 h and incubated overnight at 4°C with alkaline phosphatase-labeled sheep anti-dig antibody (11093274910, Roche, 1:2500). After washing, enzymatic activity was detected with BCIP and NBT (0.15 mg/ml and 0.18 mg/ml, respectively; Roche) in reaction solution (0.1 M Tris pH 9.5, 50 mM $MgCl_2$, 0.1 M NaCl, 0.1%Tween-20). For immuno-*in situ* hybridization double staining, sections were incubated with antibodies after developing the DIG *in situ* hybridization reaction.

β-Gal activity was developed with X-gal using a standard technique (Gosgnach et al., 2006).

Images were captured by digital camera on Zeiss Axioplan microscope for brightfield or using Zeiss LSM 510 Meta and Zeiss LSM 880 confocal microscopes and assembled using Zeiss ZEN, Adobe Photoshop and Adobe Illustrator.

Quantification and statistical analyses

Quantification and analyses were performed on thoracic and upper lumbar spinal cord segments. Cell numbers are expressed per hemisection. The number of sections and embryos analyzed are indicated in the corresponding figure legend. For cell density maps and polar graphs, photos were aligned, the scatter plots with the position of cells were recorded with ImageJ and heat maps were constructed using a MATLAB script (MathWorks). Differences between groups were evaluated by non-parametric Mann–Whitney U test or Kruskal–Wallis analysis of variance with post-hoc Dunn's Multiple Comparison test (GraphPad Software). Results are presented as mean+s.d. and differences were considered statistically significant when $P<0.05$.

Acknowledgements

We thank Tom Jessell, Martyn Goulding, Jonas Frisén and Magdalena Gotz for mice; Flavio de Souza, Pablo Vazquez, Martyn Goulding, Tom Jessell, Fred Gage, Patricia Mathieu, Ana Adamo and Fernando Pitossi for antibodies or probes, and Miguel Maroto for sharing Ly411575. We deeply thank Abel Carcagno and Daniela Di Bella for insights and kind collaboration, members of Alejandro Schinder lab for discussions, Joselina Berti for revision of the manuscript, and staff of the Animal and Imaging facilities for their support.

Competing interests

The authors declare no competing or financial interests.

Author contributions

Conceptualization: G.M.L.; Formal analysis: M.M.S., G.M.L.; Investigation: M.M.S., C.A.C., G.M.L.; Writing - original draft: M.M.S., G.M.L.; Writing - review & editing: M.M.S., C.A.C., G.M.L.; Supervision: G.M.L.; Funding acquisition: G.M.L.

Funding

This work was supported by the Agencia Nacional de Promoción Científica y Tecnológica of Argentina (PICT2014-1821 and PICT2017-0297 to G.M.L.). M.M.S. and C.A.C. were sponsored by fellowships from the Consejo Nacional de Investigaciones Científicas y Técnicas (CONICET). G.M.L. is investigator of CONICET.

References

Allen, N. J. and Eroglu, C. (2017). Cell biology of astrocyte-synapse interactions. *Neuron* **96**, 697-708. doi:10.1016/j.neuron.2017.09.056

Andersen, J., Thom, N., Shadrach, J. L., Chen, X., Amin, N. D., Yoon, S.-J., Greenleaf, W. J., Müller, F., Paşca, A. M., Kaltschmidt, J. A. et al. (2021). Landscape of human spinal cord cell type diversity at midgestation. *bioRxiv, 2021.2012.2029.473693*. doi:10.1101/2021.12.29.473693

Bahney, J. and von Bartheld, C. S. (2018). The cellular composition and glia-neuron ratio in the spinal cord of a human and a nonhuman primate: comparison with other species and brain regions. *Anat. Rec.* **301**, 697-710. doi:10.1002/ar.23728

Balaskas, N., Ribeiro, A., Panovska, J., Dessaud, E., Sasai, N., Page, K. M., Briscoe, J. and Ribes, V. (2012). Gene regulatory logic for reading the Sonic Hedgehog signaling gradient in the vertebrate neural tube. *Cell* **148**, 273-284. doi:10.1016/j.cell.2011.10.047

Barres, B. A. (2008). The mystery and magic of glia: a perspective on their roles in health and disease. *Neuron* **60**, 430-440. doi:10.1016/j.neuron.2008.10.013

Barry, D. and McDermott, K. (2005). Differentiation of radial glia from radial precursor cells and transformation into astrocytes in the developing rat spinal cord. *Glia* **50**, 187-197. doi:10.1002/glia.20166

Bjugn, R. and Gundersen, H. J. (1993). Estimate of the total number of neurons and glial and endothelial cells in the rat spinal cord by means of the optical disector. *J. Comp. Neurol.* **328**, 406-414. doi:10.1002/cne.903280307

Bouvier, J., Thoby-Brisson, M., Renier, N., Dubreuil, V., Ericson, J., Champagnat, J., Pierani, A., Chédotal, A. and Fortin, G. (2010). Hindbrain interneurons and axon guidance signaling critical for breathing. *Nat. Neurosci.* **13**, 1066-1074. doi:10.1038/nn.2622

Briscoe, J., Pierani, A., Jessell, T. M. and Ericson, J. (2000). A homeodomain protein code specifies progenitor cell identity and neuronal fate in the ventral neural tube. *Cell* **101**, 435-445. doi:10.1016/S0092-8674(00)80853-3

Cai, J., Qi, Y., Hu, X., Tan, M., Liu, Z., Zhang, J., Li, Q., Sander, M. and Qiu, M. (2005). Generation of oligodendrocyte precursor cells from mouse dorsal spinal cord independent of Nkx6 regulation and Shh signaling. *Neuron* **45**, 41-53. doi:10.1016/j.neuron.2004.12.028

Carcagno, A. L., Di Bella, D. J., Goulding, M., Guillemot, F. and Lanuza, G. M. (2014). Neurogenin3 restricts serotonergic neuron differentiation to the hindbrain. *J. Neurosci.* **34**, 15223-15233. doi:10.1523/JNEUROSCI.3403-14.2014

Carlen, M., Meletis, K., Barnabé-Heider, F. and Frisen, J. (2006). Genetic visualization of neurogenesis. *Exp. Cell Res.* **312**, 2851-2859. doi:10.1016/j.yexcr.2006.05.012

Chitnis, A. B. (1995). The role of Notch in lateral inhibition and cell fate specification. *Mol. Cell. Neurosci.* **6**, 311-321. doi:10.1006/mcne.1995.1024

Clavreul, S., Abdeladim, L., Hernandez-Garzon, E., Niculescu, D., Durand, J., Ieng, S. H., Barry, R., Bonvento, G., Beaurepaire, E., Livet, J. et al. (2019). Cortical astrocytes develop in a plastic manner at both clonal and cellular levels. *Nat. Commun.* **10**, 4884. doi:10.1038/s41467-019-12791-5

Contet, C., Goulding, S. P., Kuljis, D. A. and Barth, A. L. (2016). BK channels in the central nervous system. *Int. Rev. Neurobiol.* **128**, 281-342. doi:10.1016/bs.irn.2016.04.001

de la Pompa, J. L., Wakeham, A., Correia, K. M., Samper, E., Brown, S., Aguilera, R. J., Nakano, T., Honjo, T., Mak, T. W., Rossant, J. et al. (1997). Conservation of the Notch signalling pathway in mammalian neurogenesis. *Development* **124**, 1139-1148. doi:10.1242/dev.124.6.1139

Deneen, B., Ho, R., Lukaszewicz, A., Hochstim, C. J., Gronostajski, R. M. and Anderson, D. J. (2006). The transcription factor NFIA controls the onset of gliogenesis in the developing spinal cord. *Neuron* **52**, 953-968. doi:10.1016/j.neuron.2006.11.019

Di Bella, D. J., Carcagno, A. L., Bartolomeu, M. L., Pardi, M. B., Lohr, H., Siegel, N., Hammerschmidt, M., Marín-Burgin, A. and Lanuza, G. M. (2019). Ascl1 balances neuronal versus ependymal fate in the spinal cord central canal. *Cell Rep.* **28**, 2264-2274.e3. doi:10.1016/j.celrep.2019.07.087

Dunwoodie, S. L., Henrique, D., Harrison, S. M. and Beddington, R. S. (1997). Mouse Dll3: a novel divergent Delta gene which may complement the function of other Delta homologues during early pattern formation in the mouse embryo. *Development* **124**, 3065-3076. doi:10.1242/dev.124.16.3065

Farmer, W. T., Abrahamsson, T., Chierzi, S., Lui, C., Zaelzer, C., Jones, E. V., Bally, B. P., Chen, G. G., Théroux, J. F., Peng, J. et al. (2016). Neurons diversify astrocytes in the adult brain through sonic hedgehog signaling. *Science* **351**, 849-854. doi:10.1126/science.aab3103

Filosa, J. A., Bonev, A. D., Straub, S. V., Meredith, A. L., Wilkerson, M. K., Aldrich, R. W. and Nelson, M. T. (2006). Local potassium signaling couples neuronal activity to vasodilation in the brain. *Nat. Neurosci.* **9**, 1397-1403. doi:10.1038/nn1779

Fogarty, M., Richardson, W. D. and Kessaris, N. (2005). A subset of oligodendrocytes generated from radial glia in the dorsal spinal cord. *Development* **132**, 1951-1959. doi:10.1242/dev.01777

Freeman, M. R. (2010). Specification and morphogenesis of astrocytes. *Science* **330**, 774-778. doi:10.1126/science.1190928

Fu, Y., Rusznak, Z., Herculano-Houzel, S., Watson, C. and Paxinos, G. (2013). Cellular composition characterizing postnatal development and maturation of the mouse brain and spinal cord. *Brain Struct. Funct.* **218**, 1337-1354. doi:10.1007/s00429-012-0462-x

Gaiano, N., Nye, J. S. and Fishell, G. (2000). Radial glial identity is promoted by Notch1 signaling in the murine forebrain. *Neuron* **26**, 395-404. doi:10.1016/S0896-6273(00)81172-1

García-Marquís, J. and López-Mascaraque, L. (2013). Clonal identity determines astrocyte cortical heterogeneity. *Cereb. Cortex* **23**, 1463-1472. doi:10.1093/cercor/bhs134

Ge, W.-P., Miyawaki, A., Gage, F. H., Jan, Y. N. and Jan, L. Y. (2012). Local generation of glia is a major astrocyte source in postnatal cortex. *Nature* **484**, 376-380. doi:10.1038/nature10959

Girouard, H., Bonev, A. D., Hannah, R. M., Meredith, A., Aldrich, R. W. and Nelson, M. T. (2010). Astrocytic endfoot Ca^{2+} and BK channels determine both arteriolar dilation and constriction. *Proc. Natl. Acad. Sci. USA* **107**, 3811-3816. doi:10.1073/pnas.0914722107

Gosgnach, S., Lanuza, G. M., Butt, S. J., Saueressig, H., Zhang, Y., Velasquez, T., Riethmacher, D., Callaway, E. M., Kiehn, O. and Goulding, M. (2006). V1 spinal neurons regulate the speed of vertebrate locomotor outputs. *Nature* **440**, 215-219. doi:10.1038/nature04545

Henrique, D., Adam, J., Myat, A., Chitnis, A., Lewis, J. and Ish-Horowicz, D. (1995). Expression of a Delta homologue in prospective neurons in the chick. *Nature* **375**, 787-790. doi:10.1038/375787a0

Herrero-Navarro, Á., Puche-Aroca, L., Moreno-Juan, V., Sempere-Ferràndez, A., Espinosa, A., Susín, R., Torres-Masjoan, L., Leyva-Díaz, E., Karow, M., Figueres-Oñate, M. et al. (2021). Astrocytes and neurons share region-specific transcriptional signatures that confer regional identity to neuronal reprogramming. *Sci. Adv.* **7**, eabe8978. doi:10.1126/sciadv.abe8978

Hicks, C., Johnston, S. H., diSibio, G., Collazo, A., Vogt, T. F. and Weinmaster, G. (2000). Fringe differentially modulates Jagged1 and Delta1 signalling through Notch1 and Notch2. *Nat. Cell Biol.* **2**, 515-520. doi:10.1038/35019553

Hochstim, C., Deneen, B., Lukaszewicz, A., Zhou, Q. and Anderson, D. J. (2008). Identification of positionally distinct astrocyte subtypes whose identities are specified by a homeodomain code. *Cell* **133**, 510-522. doi:10.1016/j.cell.2008.02.046

Hoffmann, S. A., Hos, D., Küspert, M., Lang, R. A., Lovell-Badge, R., Wegner, M. and Reiprich, S. (2014). Stem cell factor Sox2 and its close relative Sox3 have differentiation functions in oligodendrocytes. *Development* **141**, 39-50. doi:10.1242/dev.098418

Hyde, L. A., McHugh, N. A., Chen, J., Zhang, Q., Manfra, D., Nomeir, A. A., Josien, H., Bara, T., Clader, J. W., Zhang, L. et al. (2006). Studies to investigate the in vivo therapeutic window of the γ-secretase inhibitor N^2-[(2S)-2-(3,5-difluorophenyl)-2-hydroxyethanoyl]-N^1-[(7S)-5-methyl-6-oxo-6,7-di hydro-5H-dibenzo[b,d]azepin-7-yl]-L-alaninamide (LY411,575) in the CRND8 mouse. *J. Pharmacol. Exp. Ther.* **319**, 1133-1143. doi:10.1124/jpet.106.111716

Jessell, T. M. (2000). Neuronal specification in the spinal cord: inductive signals and transcriptional codes. *Nat. Rev. Genet.* **1**, 20-29. doi:10.1038/35049541

Kakuda, S. and Haltiwanger, R. S. (2017). Deciphering the fringe-mediated Notch code: identification of activating and inhibiting sites allowing discrimination between ligands. *Dev. Cell* **40**, 193-201. doi:10.1016/j.devcel.2016.12.013

Kang, P., Lee, H. K., Glasgow, S. M., Finley, M., Donti, T., Gaber, Z. B., Graham, B. H., Foster, A. E., Novitch, B. G., Gronostajski, R. M. et al. (2012). Sox9 and NFIA coordinate a transcriptional regulatory cascade during the initiation of gliogenesis. *Neuron* **74**, 79-94. doi:10.1016/j.neuron.2012.01.024

Kelley, K. W., Ben Haim, L., Schirmer, L., Tyzack, G. E., Tolman, M., Miller, J. G., Tsai, H.-H., Chang, S. M., Molofsky, A. V., Yang, Y. et al. (2018). Kir4.1-dependent astrocyte-fast motor neuron interactions are required for peak strength. *Neuron* **98**, 306-319.e7. doi:10.1016/j.neuron.2018.03.010

Kong, J. H., Yang, L., Dessaud, E., Chuang, K., Moore, D. M., Rohatgi, R., Briscoe, J. and Novitch, B. G. (2015). Notch activity modulates the responsiveness of neural progenitors to sonic hedgehog signaling. *Dev. Cell* **33**, 373-387. doi:10.1016/j.devcel.2015.03.005

Lai, H. C., Seal, R. P. and Johnson, J. E. (2016). Making sense out of spinal cord somatosensory development. *Development* **143**, 3434-3448. doi:10.1242/dev.139592

Lanuza, G. M., Gosgnach, S., Pierani, A., Jessell, T. M. and Goulding, M. (2004). Genetic identification of spinal interneurons that coordinate left-right locomotor activity necessary for walking movements. *Neuron* **42**, 375-386. doi:10.1016/S0896-6273(04)00249-1

Lek, M., Dias, J. M., Marklund, U., Uhde, C. W., Kurdija, S., Lei, Q., Sussel, L., Rubenstein, J. L., Matise, M. P., Arnold, H. H. et al. (2010). A homeodomain feedback circuit underlies step-function interpretation of a Shh morphogen gradient during ventral neural patterning. *Development* **137**, 4051-4060. doi:10.1242/dev.054288

Lindsell, C. E., Boulter, J., diSibio, G., Gossler, A. and Weinmaster, G. (1996). Expression patterns of Jagged, Delta1, Notch1, Notch2, and Notch3 genes identify ligand-receptor pairs that may function in neural development. *Mol. Cell. Neurosci.* **8**, 14-27. doi:10.1006/mcne.1996.0040

Liu, X., Zhang, Z., Guo, W., Burnstock, G., He, C. and Xiang, Z. (2013). The superficial glia limitans of mouse and monkey brain and spinal cord. *Anat. Rec.* **296**, 995-1007. doi:10.1002/ar.22717

Liuzzi, F. J. and Miller, R. H. (1987). Radially oriented astrocytes in the normal adult rat spinal cord. *Brain Res.* **403**, 385-388. doi:10.1016/0006-8993(87)90081-3

Louvi, A. and Artavanis-Tsakonas, S. (2006). Notch signalling in vertebrate neural development. *Nat. Rev. Neurosci.* **7**, 93-102. doi:10.1038/nrn1847

Lu, Q. R., Yuk, D., Alberta, J. A., Zhu, Z., Pawlitzky, I., Chan, J., McMahon, A. P., Stiles, C. D. and Rowitch, D. H. (2000). Sonic hedgehog—regulated oligodendrocyte lineage genes encoding bHLH proteins in the mammalian central nervous system. *Neuron* **25**, 317-329. doi:10.1016/S0896-6273(00)80897-1

Lu, D. C., Niu, T. and Alaynick, W. A. (2015). Molecular and cellular development of spinal cord locomotor circuitry. *Front. Mol. Neurosci.* **8**, 25. doi:10.3389/fnmol.2015.00025

Lütolf, S., Radtke, F., Aguet, M., Suter, U. and Taylor, V. (2002). Notch1 is required for neuronal and glial differentiation in the cerebellum. *Development* **129**, 373-385. doi:10.1242/dev.129.2.373

Madisen, L., Zwingman, T. A., Sunkin, S. M., Oh, S. W., Zariwala, H. A., Gu, H., Ng, L. L., Palmiter, R. D., Hawrylycz, M. J., Jones, A. R. et al. (2010). A robust and high-throughput Cre reporting and characterization system for the whole mouse brain. *Nat. Neurosci.* **13**, 133-140. doi:10.1038/nn.2467

Marklund, U., Hansson, E. M., Sundström, E., de Angelis, M. H., Przemeck, G. K., Lendahl, U., Muhr, J. and Ericson, J. (2010). Domain-specific control of neurogenesis achieved through patterned regulation of Notch ligand expression. *Development* **137**, 437-445. doi:10.1242/dev.036806

McMahon, S. S. and McDermott, K. W. (2001). Proliferation and migration of glial precursor cells in the developing rat spinal cord. *J. Neurocytol.* **30**, 821-828. doi:10.1023/A:1019693421778

McMahon, S. S. and McDermott, K. W. (2002). Morphology and differentiation of radial glia in the developing rat spinal cord. *J. Comp. Neurol.* **454**, 263-271. doi:10.1002/cne.10427

Molofsky, A. V., Kelley, K. W., Tsai, H. H., Redmond, S. A., Chang, S. M., Madireddy, L., Chan, J. R., Baranzini, S. E., Ullian, E. M. and Rowitch, D. H. (2014). Astrocyte-encoded positional cues maintain sensorimotor circuit integrity. *Nature* **509**, 189-194. doi:10.1038/nature13161

Mori, T., Tanaka, K., Buffo, A., Wurst, W., Kuhn, R. and Götz, M. (2006). Inducible gene deletion in astroglia and radial glia–a valuable tool for functional and lineage analysis. *Glia* **54**, 21-34. doi:10.1002/glia.20350

Muroyama, Y., Fujiwara, Y., Orkin, S. H. and Rowitch, D. H. (2005). Specification of astrocytes by bHLH protein SCL in a restricted region of the neural tube. *Nature* **438**, 360-363. doi:10.1038/nature04139

Myat, A., Henrique, D., Ish-Horowicz, D. and Lewis, J. (1996). A chick homologue of serrate and its relationship with Notch and Delta homologues during central neurogenesis. *Dev. Biol.* **174**, 233-247. doi:10.1006/dbio.1996.0069

Nadarajah, B., Brunstrom, J. E., Grutzendler, J., Wong, R. O. and Pearlman, A. L. (2001). Two modes of radial migration in early development of the cerebral cortex. *Nat. Neurosci.* **4**, 143-150. doi:10.1038/83967

Namihira, M., Kohyama, J., Semi, K., Sanosaka, T., Deneen, B., Taga, T. and Nakashima, K. (2009). Committed neuronal precursors confer astrocytic potential on residual neural precursor cells. *Dev. Cell* **16**, 245-255. doi:10.1016/j.devcel.2008.12.014

Oberheim, N. A., Goldman, S. A. and Nedergaard, M. (2012). Heterogeneity of astrocytic form and function. *Methods Mol. Biol.* **814**, 23-45. doi:10.1007/978-1-61779-452-0_3

Pakan, J. M. and McDermott, K. W. (2014). A method to investigate radial glia cell behavior using two-photon time-lapse microscopy in an ex vivo model of spinal cord development. *Front. Neuroanat.* **8**, 22. doi:10.3389/fnana.2014.00022

Park, H. C. and Appel, B. (2003). Delta-Notch signaling regulates oligodendrocyte specification. *Development* **130**, 3747-3755. doi:10.1242/dev.00576

Parks, A. L. and Curtis, D. (2007). Presenilin diversifies its portfolio. *Trends Genet.* **23**, 140-150. doi:10.1016/j.tig.2007.01.008

Peco, E., Davla, S., Camp, D., Stacey, M., Landgraf, M. and van Meyel, D. J. (2016). Drosophila astrocytes cover specific territories of the CNS neuropil and are instructed to differentiate by Prospero, a key effector of Notch. *Development* **143**, 1170-1181. doi:10.1242/dev.133165

Peters, A., Palay, S. L. and Webster, H. F. (1991). *The Fine Structure of the Nervous System: Neurons and Their Supporting Cells*. Oxford University Press.

Petit, A., Sanders, A. D., Kennedy, T. E., Tetzlaff, W., Glattfelder, K. J., Dalley, R. A., Puchalski, R. B., Jones, A. R. and Roskams, A. J. (2011). Adult spinal cord radial glia display a unique progenitor phenotype. *PLoS One* **6**, e24538. doi:10.1371/journal.pone.0024538

Pierani, A., Moran-Rivard, L., Sunshine, M. J., Littman, D. R., Goulding, M. and Jessell, T. M. (2001). Control of interneuron fate in the developing spinal cord by the progenitor homeodomain protein Dbx1. *Neuron* **29**, 367-384. doi:10.1016/S0896-6273(01)00212-4

Pierfelice, T., Alberi, L. and Gaiano, N. (2011). Notch in the vertebrate nervous system: an old dog with new tricks. *Neuron* **69**, 840-855. doi:10.1016/j.neuron.2011.02.031

Pringle, N. P., Yu, W.-P., Howell, M., Colvin, J. S., Ornitz, D. M. and Richardson, W. D. (2003). Fgfr3 expression by astrocytes and their precursors: evidence that astrocytes and oligodendrocytes originate in distinct neuroepithelial domains. *Development* **130**, 93-102. doi:10.1242/dev.00184

Ramos, C., Rocha, S., Gaspar, C. and Henrique, D. (2010). Two Notch ligands, Dll1 and Jag1, are differently restricted in their range of action to control neurogenesis in the mammalian spinal cord. *PLoS One* **5**, e15515. doi:10.1371/journal.pone.0015515

Rowitch, D. H. and Kriegstein, A. R. (2010). Developmental genetics of vertebrate glial-cell specification. *Nature* **468**, 214-222. doi:10.1038/nature09611

Sagner, A. and Briscoe, J. (2019). Establishing neuronal diversity in the spinal cord: a time and a place. *Development* **146**, dev182154. doi:10.1242/dev.182154

Selkoe, D. and Kopan, R. (2003). Notch and Presenilin: regulated intramembrane proteolysis links development and degeneration. *Annu. Rev. Neurosci.* **26**, 565-597. doi:10.1146/annurev.neuro.26.041002.131334

Shen, J., Bronson, R. T., Chen, D. F., Xia, W., Selkoe, D. J. and Tonegawa, S. (1997). Skeletal and CNS defects in Presenilin-1-deficient mice. *Cell* **89**, 629-639. doi:10.1016/S0092-8674(00)80244-5

Shen, Z., Lin, Y., Yang, J., Jorg, D. J., Peng, Y., Zhang, X., Xu, Y., Hernandez, L., Ma, J., Simons, B. D. et al. (2021). Distinct progenitor behavior underlying neocortical gliogenesis related to tumorigenesis. *Cell Rep.* **34**, 108853. doi:10.1016/j.celrep.2021.108853

Shibata, T., Yamada, K., Watanabe, M., Ikenaka, K., Wada, K., Tanaka, K. and Inoue, Y. (1997). Glutamate transporter GLAST is expressed in the radial glia-astrocyte lineage of developing mouse spinal cord. *J. Neurosci.* **17**, 9212-9219. doi:10.1523/JNEUROSCI.17-23-09212.1997

Skaggs, K., Martin, D. M. and Novitch, B. G. (2011). Regulation of spinal interneuron development by the Olig-related protein Bhlhb5 and Notch signaling. *Development* **138**, 3199-3211. doi:10.1242/dev.057281

Stolt, C. C., Lommes, P., Sock, E., Chaboissier, M. C., Schedl, A. and Wegner, M. (2003). The Sox9 transcription factor determines glial fate choice in the developing spinal cord. *Genes Dev.* **17**, 1677-1689. doi:10.1101/gad.259003

Tabata, H. (2015). Diverse subtypes of astrocytes and their development during corticogenesis. *Front. Neurosci.* **9**, 114. doi:10.3389/fnins.2015.00114

Taylor, M. K., Yeager, K. and Morrison, S. J. (2007). Physiological Notch signaling promotes gliogenesis in the developing peripheral and central nervous systems. *Development* **134**, 2435-2447. doi:10.1242/dev.005520

Tien, A. C., Tsai, H. H., Molofsky, A. V., McMahon, M., Foo, L. C., Kaul, A., Dougherty, J. D., Heintz, N., Gutmann, D. H., Barres, B. A. et al. (2012). Regulated temporal-spatial astrocyte precursor cell proliferation involves BRAF signalling in mammalian spinal cord. *Development* **139**, 2477-2487. doi:10.1242/dev.077214

Tsai, H. H., Li, H., Fuentealba, L. C., Molofsky, A. V., Taveira-Marques, R., Zhuang, H., Tenney, A., Murnen, A. T., Fancy, S. P., Merkle, F. et al. (2012). Regional astrocyte allocation regulates CNS synaptogenesis and repair. *Science* **337**, 358-362. doi:10.1126/science.1222381

Vallstedt, A., Klos, J. M. and Ericson, J. (2005). Multiple dorsoventral origins of oligodendrocyte generation in the spinal cord and hindbrain. *Neuron* **45**, 55-67. doi:10.1016/j.neuron.2004.12.026

Verkhratsky, A. and Nedergaard, M. (2018). Physiology of Astroglia. *Physiol. Rev.* **98**, 239-389. doi:10.1152/physrev.00042.2016

Vue, T. Y., Kim, E. J., Parras, C. M., Guillemot, F. and Johnson, J. E. (2014). Ascl1 controls the number and distribution of astrocytes and oligodendrocytes in the gray matter and white matter of the spinal cord. *Development* **141**, 3721-3731. doi:10.1242/dev.105270

Yang, L. T., Nichols, J. T., Yao, C., Manilay, J. O., Robey, E. A. and Weinmaster, G. (2005). Fringe glycosyltransferases differentially modulate Notch1 proteolysis induced by Delta1 and Jagged1. *Mol. Biol. Cell* **16**, 927-942. doi:10.1091/mbc.e04-07-0614

Zagoraiou, L., Akay, T., Martin, J. F., Brownstone, R. M., Jessell, T. M. and Miles, G. B. (2009). A cluster of cholinergic premotor interneurons modulates mouse locomotor activity. *Neuron* **64**, 645-662. doi:10.1016/j.neuron.2009.10.017

Zhao, X., Chen, Y., Zhu, Q., Huang, H., Teng, P., Zheng, K., Hu, X., Xie, B., Zhang, Z., Sander, M. et al. (2014). Control of astrocyte progenitor specification, migration and maturation by Nkx6.1 homeodomain transcription factor. *PLoS One* **9**, e109171. doi:10.1371/journal.pone.0109171

Zhou, Q., Wang, S. and Anderson, D. J. (2000). Identification of a novel family of oligodendrocyte lineage-specific basic helix-loop-helix transcription factors. *Neuron* **25**, 331-343. doi:10.1016/S0896-6273(00)80898-3